

Probing “Generalized Parton Distributions” with JLab at 12 GeV

S. Stepanyan

Thomas Jefferson National Accelerator Facility, Newport News, VA 23606, USA

Christopher Newport University, Newport News, VA 23606, USA

Abstract

We discuss plans for Jefferson Lab to explore GPDs in hard exclusive reactions. A broad experimental program is proposed with up to 11 GeV polarized electron beams. Such an upgraded CEBAF, with high precision, and high performance detectors, will be a suitable place to study deep virtual production of mesons and photons in the range of $Q^2 < 8 \text{ GeV}/c^2$. These studies are proposed as a key program for the Hall B CLAS detector.

1 Introduction

One of the fundamental topics of modern high energy physics is the understanding of nucleon structure. Studies with leptonic beams in the deep inelastic scattering region (DIS) led to discovery of the quark-gluon structure of the nucleon. It was found, for example, that quarks carry about half of the nucleon momentum, and about 25% of the spin of the nucleon.

To have a more complete picture of nucleon structure, new information is needed, particularly information on quark-quark and quark-gluon interactions in the nucleon. Recent developments in the theory showed that such information can be obtained in hard exclusive leptonproduction experiments. Formalism, developed by Ji [1], Radyushkin [2] and others, for the QCD description of hard exclusive reactions introduces new Generalized Parton Distributions, (or Skewed Parton Distributions, or Off-Forward Parton Distributions). GPDs contain information on quark-quark correlations, on transverse and angular momentum distributions, and provide a unified description of a wide range of inclusive and exclusive reactions.

A broad program for studying GPDs with longitudinally polarized electron beams is proposed for JLab with the upgraded 12 GeV machine [3]. First explorations of the most promising channels will begin even at lower beam energies.

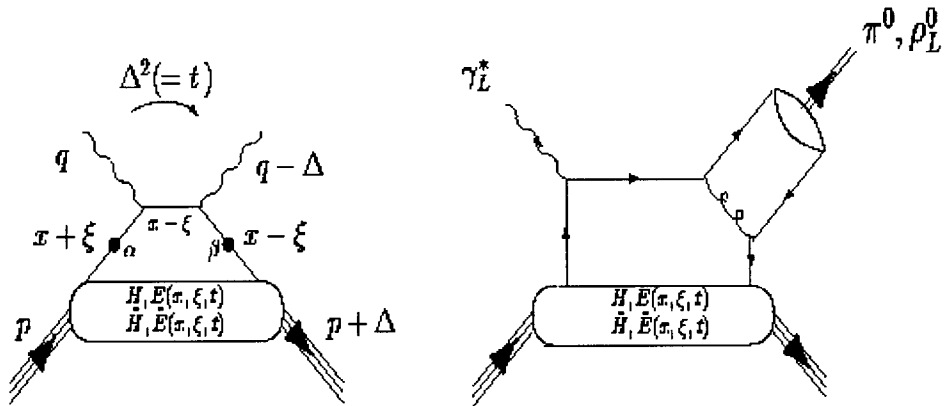


Figure 1: Handbag diagrams corresponding to Deep Virtual Compton Scattering (a) and Deep Virtual Meson Production (b).

In this report an overview of the experimental program proposed for CEBAF 12 GeV upgrade and some details of key reactions are presented.

2 Physics Motivation

It has been shown that in leading-order pQCD the amplitude of Deep Virtual Meson Production with longitudinally polarized photons (generally called Deep Exclusive Scattering, DES), and the amplitude of Deep Virtual Compton Scattering (DVCS) in the forward direction can be factorized into a hard-scattering part (exactly calculable in pQCD) and a non-perturbative nucleon structure part as illustrated in Figure 1. In these so-called “handbag” diagrams, the lower blob represents the structure of the nucleon and can be parametrized in terms of four structure functions, known as the GPDs.

The GPDs are defined as $H, \tilde{H}, E,$ and \tilde{E} , and depend upon three kinematic variables: $x, \xi,$ and t . x is the momentum fraction of the struck quark in the quark loop and, as such, is not directly accessible experimentally. ξ is the longitudinal-momentum fraction of the transfer Δ with $\xi = x_B/(2 - x_B)$. $t = \Delta^2$ is the standard momentum transfer between the final-state meson and the virtual photon. H and E are spin-independent and \tilde{H} and \tilde{E} are spin-dependent functions. The GPDs are also quark flavor dependent.

The GPDs H and \tilde{H} are generalizations of the parton distributions measured in deep inelastic scattering. In the forward direction (defined by $q = q'$), H reduces to the quark distribution $q(x)$ and \tilde{H} to the quark-helicity distribution

$\Delta q(x)$ measured in deep inelastic scattering. Furthermore, at finite momentum transfer, there are model-independent sum rules that relate the first moments of these GPDs to the standard elastic form factors. Also Ji [1] has shown that the second moment of these GPDs gives access to the sum of the quark spin and the quark orbital angular momentum to the nucleon spin.

3 Experimental Program

The proposed experimental program includes production of mesons in Deep Exclusive Scattering (DES) and the Deep Virtual Compton Scattering (DVCS). Systematic studies are feasible in a wide range of kinematics, as shown in Figure 2. The interests are X_B , Q^2 and t dependence of exclusive reactions like:

$$\begin{aligned} \vec{e}p &\rightarrow ep\gamma \\ ep &\rightarrow ep(\rho^{+,0,-}) \\ ep &\rightarrow ep(\pi^{+,0,-}) \\ ep &\rightarrow e\Delta(\pi^{+,0,-}) \\ ep &\rightarrow e(\Lambda\Sigma)K \end{aligned}$$

In the case of DES the GPD formalism is valid for longitudinally polarized photons and therefore a L/T separation is essential. In the scaling regime cross sections for DES should scale as $\sigma_L \sim 1/Q^6$, for DVCS $\sigma \sim 1/Q^4$. It is important to measure cross sections and the spin observables. These will give access to the real and the imaginary parts of GPD amplitudes.

The spin dependent (\tilde{H} and \tilde{E}) and the spin independent (H and E) GPDs can be separated by measuring pseudo-scalar and vector meson productions, respectively. Comparison of production of different final mesonic states ($\rho^{+,0,-}$, ω , $\pi^{+,0,-}$, η , etc) will allow quark flavor decomposition of GPDs.

The CLAS detector in Hall B will allow simultaneous measurements of many multiparticle final states. Currently CLAS has been operated at luminosity $L = 10^{34} \text{ cm}^{-2} \text{ sec}^{-1}$ and has wide angular coverage of final state particles (see Figure 3.a). The upgraded CLAS will have increased acceptance and improved resolution in the forward scattering region, and will have the capability to run at luminosity $L = 10^{35} \text{ cm}^{-2} \text{ sec}^{-1}$, Figure 3.b [4]. High luminosity is very important for high Q^2 exclusive measurements.

In the following chapter the experimental expectations of some of the key channels are presented.

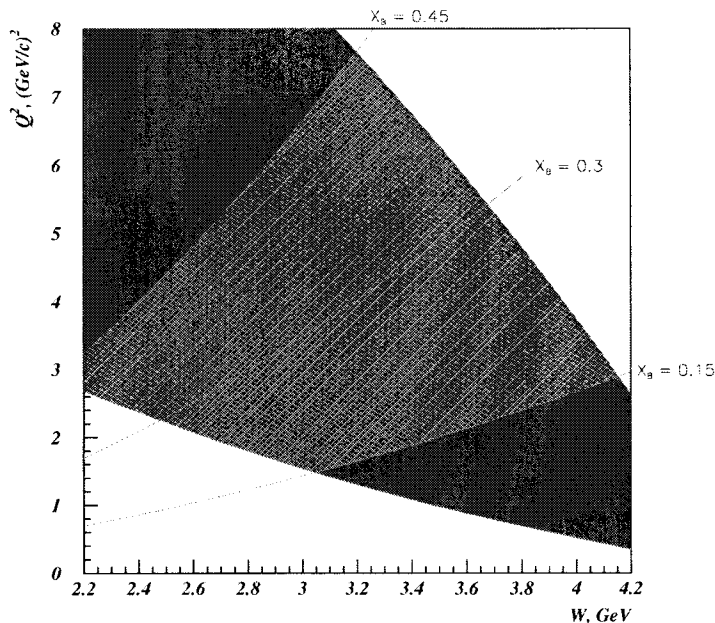


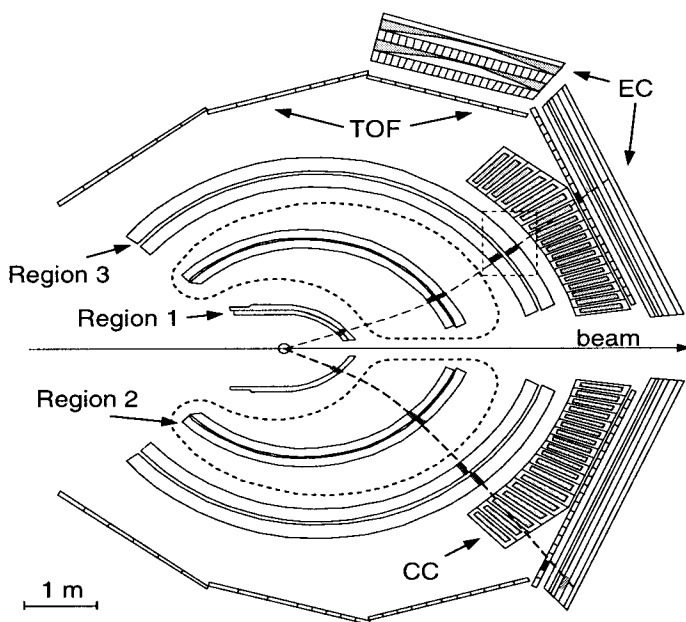
Figure 2: The accessible range of Q^2 and W with 11 GeV beam energy. Lines represent fixed values of X_B .

3.1 Deep exclusive ρ^0 production

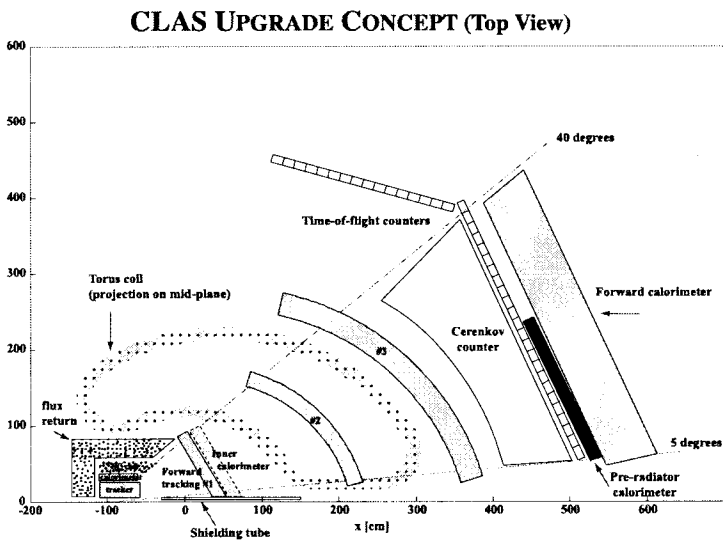
The cross section of ρ_L^0 production is sensitive to the H and E GPDs. In the past, the total cross section of longitudinally polarized ρ^0 s has been measured in a number of experiments [6], [7], [8]. The data suggest that at high energies and Q^2 above a few GeV/c^2 the perturbative two gluon exchange mechanism (PTGEM) is dominant. However in the low energy region ($W \leq 10 \text{ GeV}$) this mechanism significantly underestimates the data (see Figure 4). It is evident that at $W \sim 3 \text{ GeV}$ to 4 GeV , the quark exchange mechanism (QEM) becomes the dominant contribution. This region will be accessible with the upgrade of CEBAF accelerator.

The analysis of angular distributions of charged pions, after ρ^0 decay, will allow reliable L/T separation assuming S-channel helicity conservation.

To estimate the expected sensitivity at 11 GeV, pseudo-data were generated according to the L/T ratio shown in Figure 5. It was assumed that $\sigma_L \sim 1/Q^6$ and $\sigma_T \sim 1/Q^8$. The detector response was simulated according to the design characteristics. In Figure 6 the reconstructed longitudinal, transverse and the total cross sections for exclusive ρ^0 production are shown. Errors correspond to 500 hours of CLAS running at a luminosity $L = 10^{35} \text{ cm}^{-2} \text{ sec}^{-1}$. The obtained slopes of the Q^2 dependence reproduce the generated spectra (lines on the plot) well.



a) Current CLAS detector. Operating luminosity $L = 10^{34} \text{ cm}^{-2} \text{ sec}^{-1}$, detection angular ranges: electrons $\theta = 10^\circ - 50^\circ$, charged hadrons $\theta = 8^\circ - 135^\circ$, neutrals $\theta = 8^\circ - 45^\circ$.



b) CLAS upgrade concept. Design luminosity $L = 10^{35} \text{ cm}^{-2} \text{ sec}^{-1}$, detection angular ranges: electrons $\theta = 5^\circ - 40^\circ$, charged hadrons $\theta = 5^\circ - 110^\circ$, neutrals $\theta = 5^\circ - 110^\circ$.

Figure 3: Top view of current and upgraded CLAS

$$\gamma^* + p \rightarrow \rho_L^0 + p : Q^2 = 6, 9, 17 \text{ GeV}^2$$

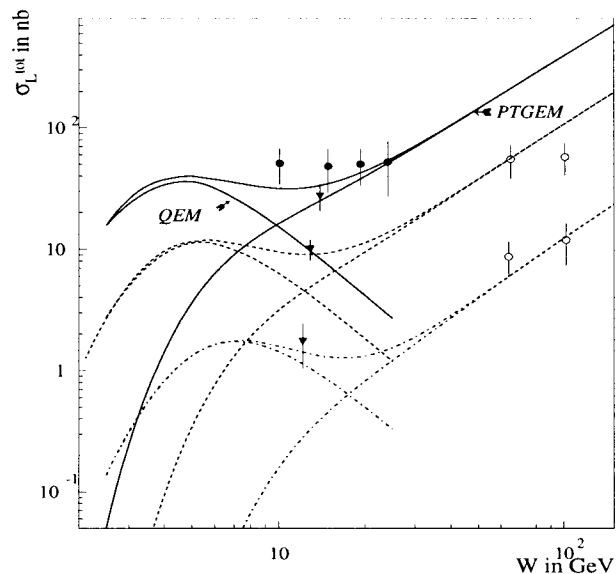


Figure 4: Total longitudinal cross section for ρ_L^0 electroproduction as calculated in [5]. Data from NMC [6] (triangles) at $Q^2 = 5.5 \text{ GeV}/c^2$ (highest point), $8.8 \text{ GeV}/c^2$ and $16.9 \text{ GeV}/c^2$ (lowest point), E665 [7] (black circles) at $Q^2 = 5.6 \text{ GeV}/c^2$ and ZEUS [8] (open circles) at $Q^2 = 8.8 \text{ GeV}/c^2$ (upper points) and $16.9 \text{ GeV}/c^2$ (lower points). Calculations are shown at $Q^2 = 6 \text{ GeV}/c^2$ (full lines), $Q^2 = 9 \text{ GeV}/c^2$ (dashed lines) and $Q^2 = 17 \text{ GeV}/c^2$ (dashed-dotted lines). The curves which grow at high W correspond to gluon exchange whereas the curves which are peaked below $W \approx 10 \text{ GeV}$ correspond to quark exchange. The incoherent sum of both mechanisms is also shown.

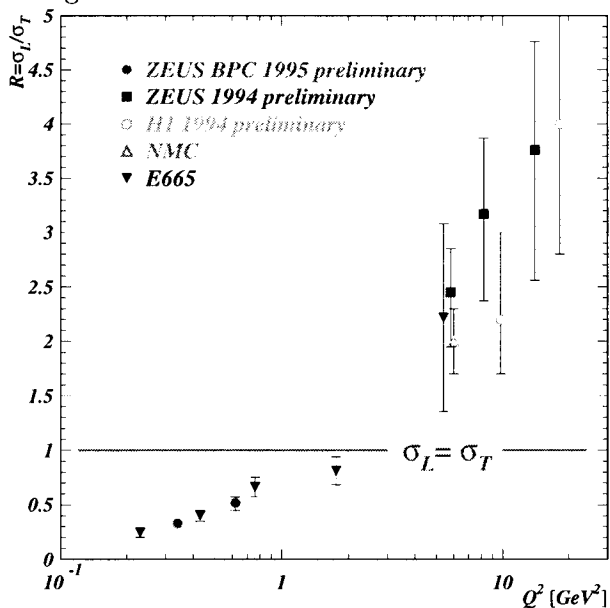


Figure 5: L/T ratio for exclusive ρ^0 electroproduction as a function of Q^2 .

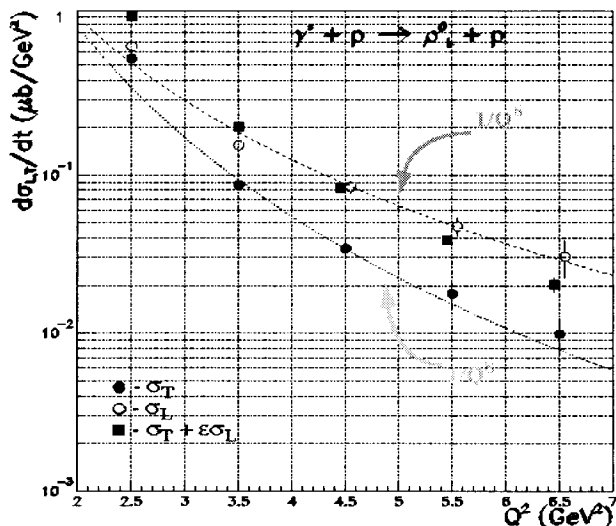


Figure 6: Reconstructed from pseudo-data σ_L , σ_T and total cross section of ρ^0 electroproduction. Lines are simulated Q^2 dependences for σ_L and σ_T . Error bars correspond to 500 hours of CLAS running at luminosity $L = 10^{35} \text{ cm}^{-2} \text{ sec}^{-1}$.

3.2 Deep exclusive π^+ production

The cross section of π^+ production is sensitive to the spin-dependent GPDs, \tilde{E} and \tilde{H} . There are two diagrams contributing to π^+ production. First is the pseudo-vector (PV) contribution, when a virtual photon interacts with a quark in a nucleon, which after gluon exchange, combines with a second quark to form the pion (see Figure 1.b). Second is the pseudoscalar (PS) contribution (pion pole), when a virtual photon knocks out a pion from the meson cloud (Figure 7). The PV mechanism is sensitive to \tilde{H} and PS is sensitive to \tilde{E} .

Relative contributions of these two diagrams depend on t and X_B . At small t and large X_B the PS contribution is large, while at large t and small X_B the PV component is dominant (see Figure 8 [9]). (Also the π^+/π^0 comparison will contribute to separation of \tilde{H} and \tilde{E} , since in the case of π^0 production there is no pion pole effect.)

For identification of the longitudinal part of the π^+ cross section Rosenbluth separation will be done using measurements at several beam energies. In Figure 9 reconstruction of cross sections from simulated pseudo-data are presented. In order to perform Rosenbluth separation pseudo-data at beam energies 6 GeV and 8 GeV are simulated. Only statistical errors are shown, corresponding to 1000 hours of running at $L = 10^{35} \text{ cm}^{-2} \text{ sec}^{-1}$.

Reasonable accuracy of separation is achievable at Q^2 up to $5.5 \text{ GeV}/c^2$. One should point out that if measurements show dominance of the longitudinal part

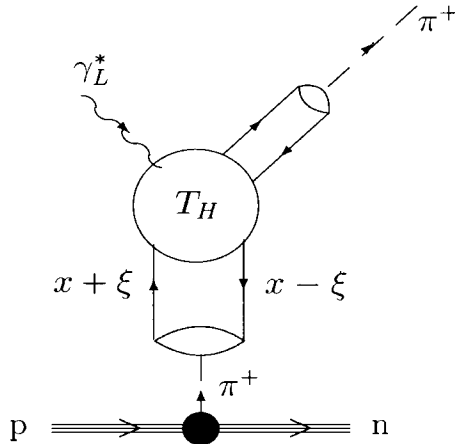


Figure 7: Pseudoscalar contribution to “hard” π^+ electroproduction. The virtual photon knocks out a pion from the meson cloud of the nucleon.

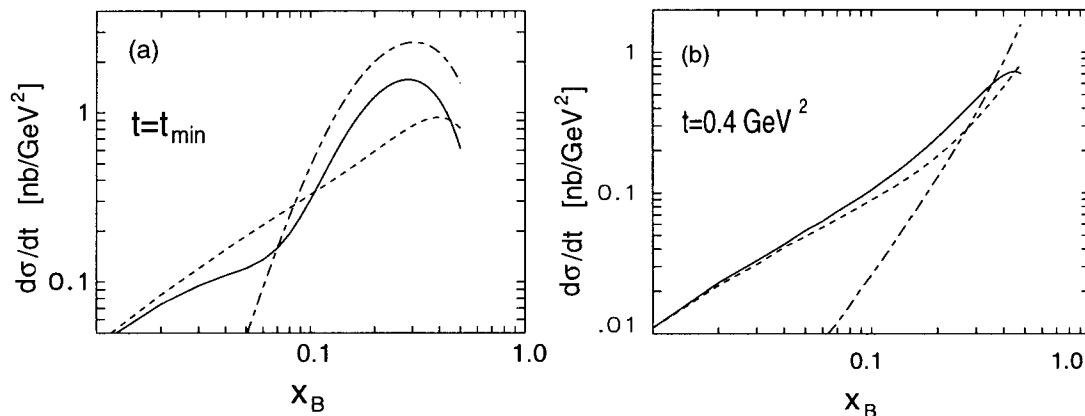


Figure 8: Cross section for exclusive π^+ production through the scattering of longitudinally polarized photons off the proton at $Q^2 = 10 \text{ GeV}/c^2$ for (a) $t = t_{\min}$ and (b) $t = -0.4 \text{ GeV}/c^2$. The dashed and dot-dashed curves show the pseudovector and pseudoscalar contributions, respectively.

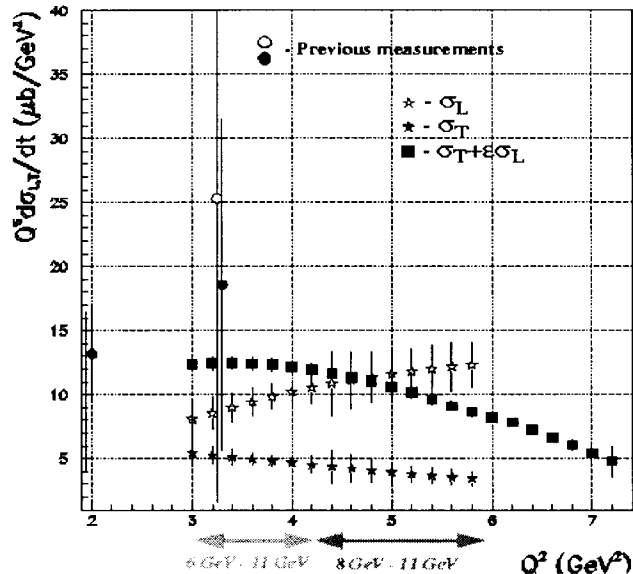


Figure 9: Separated L , T and unseparated differential cross section for π^+ production.

of the cross section at high Q^2 , then for studying GPDs the total cross section, measured with higher accuracy and higher values of Q^2 , can be used.

Using π^+ production it is possible also to measure transverse target spin asymmetry in the reaction $ep^+ \rightarrow en\pi^+$. Although CLAS will have a longitudinally polarized target, there is a transverse component to the direction of the virtual photon. Measured asymmetry will be sensitive to the product of the imaginary parts of \tilde{E} and \tilde{H} .

In Figure 10 the expected results (data point with error bars) are plotted with model calculations. Errors correspond to a 1000 hours of CLAS running at luminosity $L = 10^{35} \text{ cm}^{-2} \text{ sec}^{-1}$. There is reasonable accuracy and sensitivity for Q^2 up to $\sim 4 \text{ GeV}/c^2$.

3.3 DVCS

DVCS is the most promising channel for studying GPDs. The validity of the handbag diagram is expected to be at lower Q^2 than in the case of DES. This is supported by measurements of the $\gamma^*\gamma\pi^0$ form factor on e^-e^+ colliders. In leading order pQCD, the DVCS process and the production of π^0 by two photons, where one of the photons is highly virtual, have the same handbag diagram. In Figure 11 the recent measurements of $F_{\gamma^*\gamma\pi^0}$ from CLEO [11] are shown. The curves correspond to the leading order and the next to leading order calculations. As can be seen from the figure, $F_{\gamma^*\gamma\pi^0}$ starts to scale as $1/Q^2$ already at $Q^2 \sim 2 \text{ GeV}/c^2 - 3 \text{ GeV}/c^2$. When accounting for the internal quark motion the data are

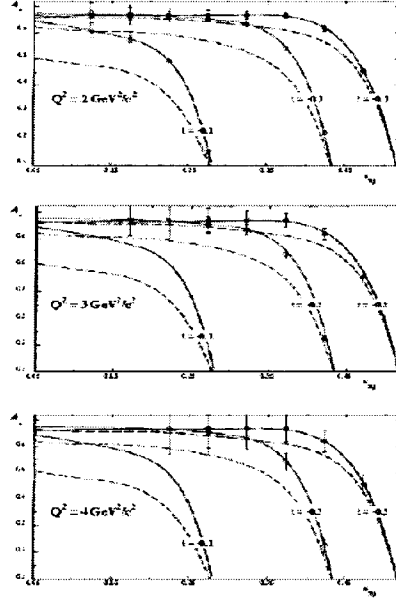


Figure 10: Transverse target asymmetry in the reaction $e\bar{p} \rightarrow en\pi^+$ as a function of X_B at different t and pseudo-data are generated assuming 1000 hours of CLAS running at luminosity $L = 10^{35} \text{ cm}^{-2} \text{ sec}^{-1}$.

well described for $Q^2 > 1 \text{ GeV}^2/c^2$

One complication with experimentally studying DVCS is the interference with the Bethe-Heitler (BH) process (see Figure 12).

$$\frac{d\sigma}{dQ^2 dX_B dt t\phi} = |T^{VCS} + T^{BH}|^2 \quad (1)$$

DVCS contributions can be extracted from measurements in various ways:

- Direct measurements of the absolute DVCS amplitude in the region where the BH contribution is small and can be neglected
- Extracting the imaginary part of the DVCS amplitude by measuring Single Spin Asymmetry (SSA) with longitudinally polarized beam
- Extracting the real part of the amplitude by measuring the beam charge asymmetry (e^- and e^+ beams)

For a complete understanding of GPDs, studies of all three processes are desirable in a wide range of kinematics.

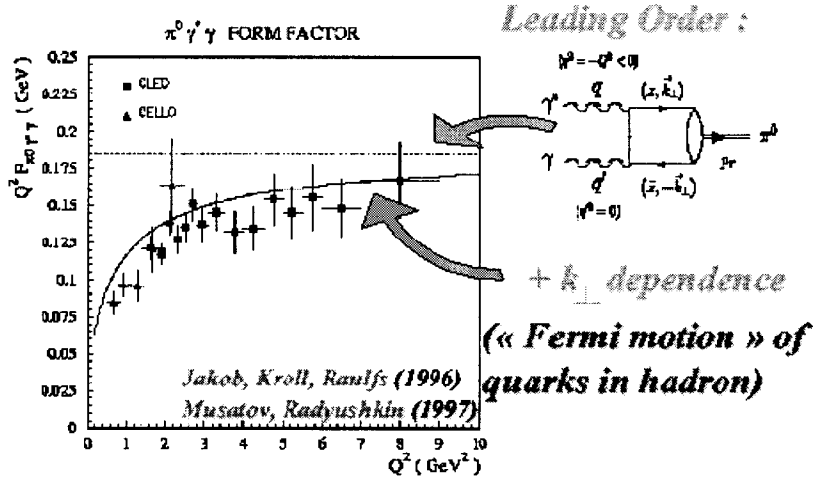


Figure 11: Experimental data on $F_{\gamma^* \gamma \pi^0}$ from [11] with predictions in the leading order and the next to leading order pQCD

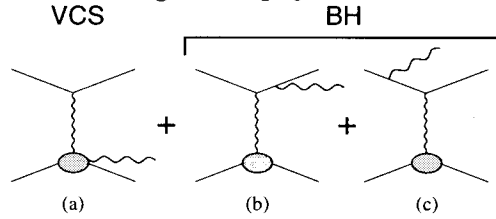


Figure 12: Feynman diagrams for VCS and Bethe-Heitler processes contributing in the amplitude of $ep \rightarrow ep\gamma$ scattering.

The first two measurements can be achieved with electron beams as will be available after the CEBAF 12 GeV upgrade, while the third one requires use of positron beams.

In Figure 13 the cross sections are shown for the DVCS and BH processes as a function of $\theta_{\gamma^* \gamma}$, the polar angle between virtual and real photons, for beam energies of 6 GeV, 12 GeV, 27 GeV and 200 GeV. Calculations are done at $Q^2 = 2.5 \text{ GeV}/c^2$ and $X_B = 0.3$ when real photons are produced in the lepton scattering plane [12]. At 12 GeV beam energy in the range of $\theta_{\gamma^* \gamma} > -2.5^\circ$ the BH contribution is large, while at $\theta_{\gamma^* \gamma} < -5^\circ$ ($-t > 0.4 \text{ GeV}/c^2$) the DVCS contribution dominates in the cross section.

The measurements of $ep \rightarrow ep\gamma$ in the range $\theta_{\gamma^* \gamma} < -5^\circ$ ($-t > 0.4 \text{ GeV}/c^2$) will be sensitive to the square of the DVCS amplitude. In Figure 14 the t -dependence of the differential cross section calculated by [12] is presented. The solid and dotted curves are calculations with different model assumptions. The points are pseudo-data generated assuming 500 hours of CLAS running at luminosity of $L = 10^{35} \text{ cm}^{-2} \text{ sec}^{-1}$. One can see reasonable sensitivity to the model assumptions at this kinematics.

The availability of the highly polarized electron beam will allow also to mea-

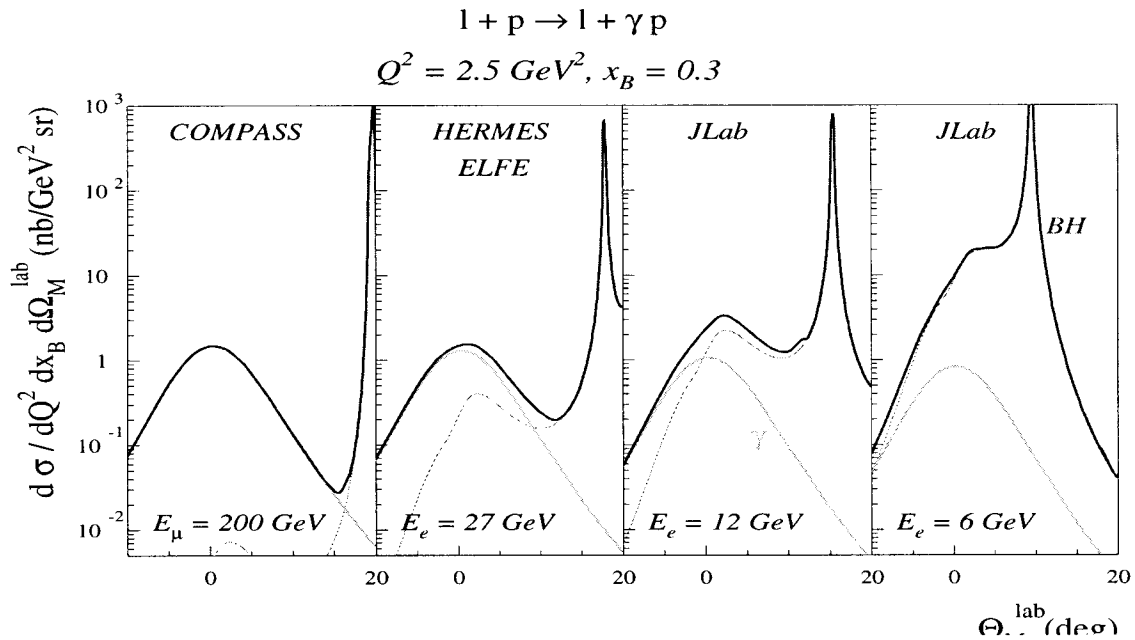


Figure 13: Cross section of $ep \rightarrow ep\gamma$ as a function of the angle between virtual and real photons at beam energies 6 GeV, 12 GeV, 27 GeV and 200 GeV. Kinematics of the reaction is fixed at $Q^2 = 2.5 \text{ GeV}^2$ and $X_B = 0.3$. The green curve is the contribution of DVCS, the red curve is Bethe-Heitler and the blue curve is the total. Cross sections are calculated according to [12].

sure the Single Spin Asymmetry (SSA) in DVCS. The asymmetry arises as a result of an interference between real and imaginary parts of the longitudinal and transverse amplitudes.

$$\frac{d^5\sigma^+}{dQ^2 dX dt d\phi} - \frac{d^5\sigma^-}{dQ^2 dX dt d\phi} \sim \text{Im}(T^{\text{VCS}}) \times \text{Re}(T^{\text{BH}}) \quad (2)$$

where “+” and “-” denote positive and negative helicities of the beam.

Similar estimations of the expected statistical errors for measurements of beam spin asymmetries with longitudinally polarized beam have been done as well. In Figure 15 the asymmetries are shown with projected (statistical) errors for 500 hours of running CLAS in the same conditions as above. The curves correspond to the different model approaches and show sensitivity to the model parameters.

4 Summary

A broad experimental program is proposed for JLab with CEBAF 12 GeV.

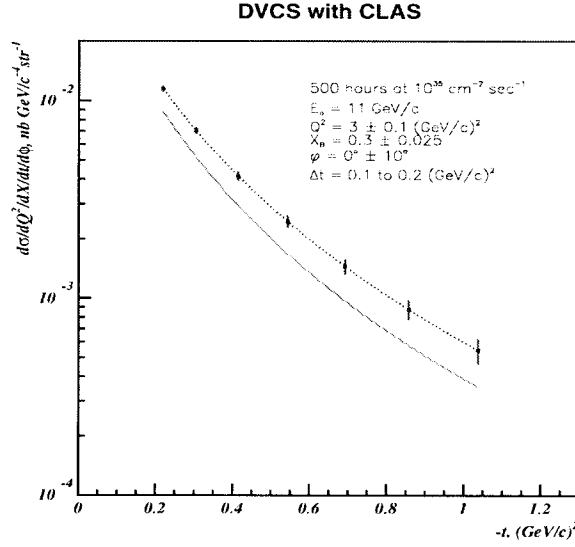


Figure 14: t -dependence of the cross section of the $ep \rightarrow ep\gamma$ process at beam energy 11 GeV. Errors are evaluated according to 500 hours of running CLAS at luminosity $10^{35} \text{ cm}^{-2} \text{ sec}^{-1}$. Pseudo-data were integrated in the bins of $Q^2 = 3 \pm 0.1 \text{ GeV}/c^2$ and $X_B = 0.3 \pm 0.025$ and $\phi_{\gamma^*\gamma} = 0 \pm 10^\circ$. The solid line is the calculation without ξ dependence. The dotted line is the calculation with ξ dependence.

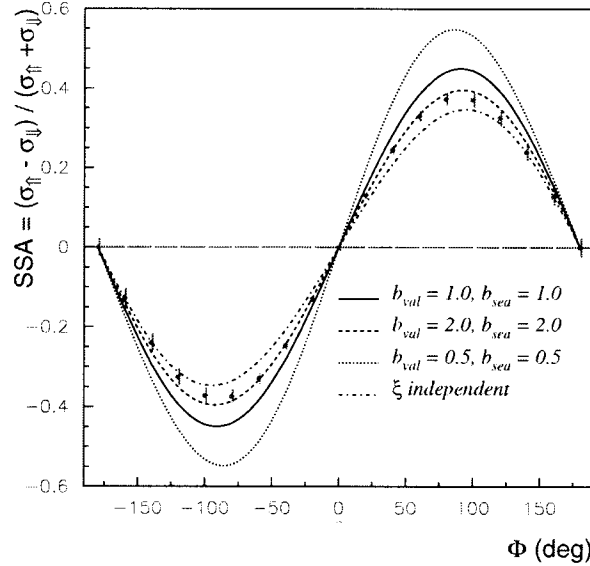


Figure 15: The Single Spin Asymmetry in the $ep \rightarrow ep\gamma$ reaction measured with longitudinally polarized 11 GeV electron beam. Points are pseudo-data generated for 500 hours of running on CLAS at luminosity $10^{35} \text{ cm}^{-2} \text{ sec}^{-1}$. Pseudo-data were integrated in the bins of $Q^2 = 3 \text{ GeV}/c^2 \pm 0.1 \text{ GeV}/c^2$ and $X_B = 0.2 \pm 0.05$ and $-t = 0.2 \pm 0.1 \text{ GeV}/c^2$.

Data on deep virtual meson and photon production will be collected in the range of Q^2 up to $8 \text{ GeV}/c^2$ and X_B from 0.1 to 0.5.

- L/T separation in the production of mesons is feasible up to $Q^2 \sim 6 \text{ GeV}/c^2$
- Unseparated cross sections can be measured up to $Q^2 \sim 8 \text{ GeV}/c^2$
- Beam asymmetry in DVCS can be measured up to $Q^2 \sim 7 \text{ GeV}/c^2$
- Target asymmetry for π^+ production is feasible at $Q^2 \sim 5 \text{ GeV}/c^2$

A large amount of data will be collected in essentially an unexplored domain. If the scaling regime is reached then measurements will have high sensitivity to GPD modes. Otherwise data will be very valuable for understanding pre-asymptotic effects.

The author thanks V. Burkert, L. Elouadrhiri and M. Guidal for help in preparing the material and for very helpful discussions. Also thanks to all authors of the proposal “Deep Virtual Electroproduction of Mesons and Photon with JLab at 12 GeV” for 12 GeV upgrade for valuable input. Many thanks to organizers of the “Second Workshop on Physics with EPIC” for an invitation to the workshop.

References

- [1] X. Ji, Phys. Rev. Lett. **78**, 610 (1997); Phys. Rev. D **55**, 7114 (1997).
- [2] A.V. Radyushkin, Phys. Lett. B **380**, 417 (1996); Phys. Rev. D **56**, 5524 (1997).
- [3] Deep Virtual Electroproduction of Mesons and Photons with JLab at 12 GeV. http://www.jlab.org/div_dept/physics_division/skewed/
- [4] Hall B plans for energy upgrade. http://www.jlab.org/div_dept/physics_division/skewed/
- [5] M. Vanderhaeghen, P.A.M. Guichon, and M. Guidal, Phys. Rev. Lett. **80**, 5064 (1998).
- [6] M. Arneodo et al., Nucl.Phys. **B429** (1994) 503.

- [7] M.R. Adams et al., Z.Phys.C **74** (1997) 237.
- [8] M. Derrick et al., Phys.Lett.B **356** (1995) 601.
- [9] L. Mankiewicz, G. Piller, and A. Radyushkin, Eur. Phys. J. C **10**, 307, (1999).
- [10] A. Radyushkin “Measuring Skewed Parton Distributions”, JLab-THY-00-DRAFT.
- [11] J. Gronberg et al. (CLEO Collaboration), Phys.Rev. **D 57**, 33 (1998)
- [12] M. Guidal “Computer Code for DVCS and BH Calculations”, Private communications.